Supporting Information for

Improved Photoresponse of UV Photodetectors by the Incorporation of Plasmonic Nanoparticles on GaN through the Resonant Coupling of Localized Surface Plasmon Resonance

Sundar Kunwar[1], Sanchaya Pandit[1], Jae-Hun Jeong[1], Jihoon Lee [1,*]

[1]Department of Electronic Engineering, College of Electronics and Information, Kwangwoon University, Nowon-gu Seoul 01897, South Korea

*Corresponding author. E-mail: jihoonlee@kw.ac.kr (Jihoon Lee)

Supplementary Figures and Tables

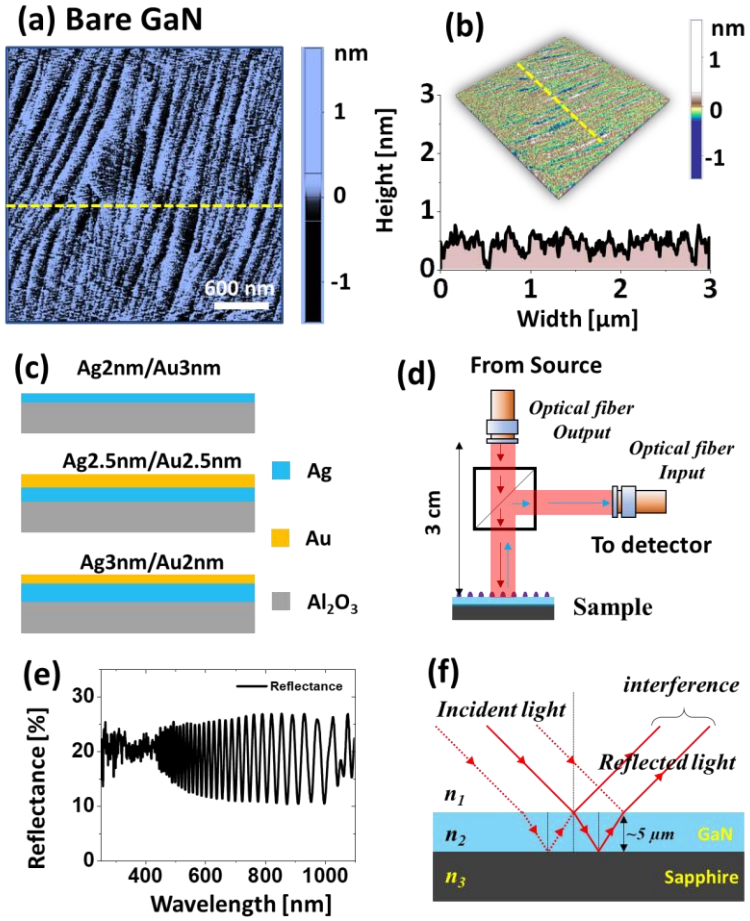

Fig. S1 a AFM images of bare GaN prior to the deposition of metallic films. **b** Corresponding AFM side-view and cross-sectional line-profile. **c** Schematic for the deposition of Ag, Au and Ag/Au bilayers for the fabrication of plasmonic NPs/GaN based UV photodetectors. **d** Schematic of UV-VIS-NIR reflectance measurement. **e** Reflectance spectra. **f** Schematic of interreference between reflected light between air/GaN and GaN/Sapphire interface

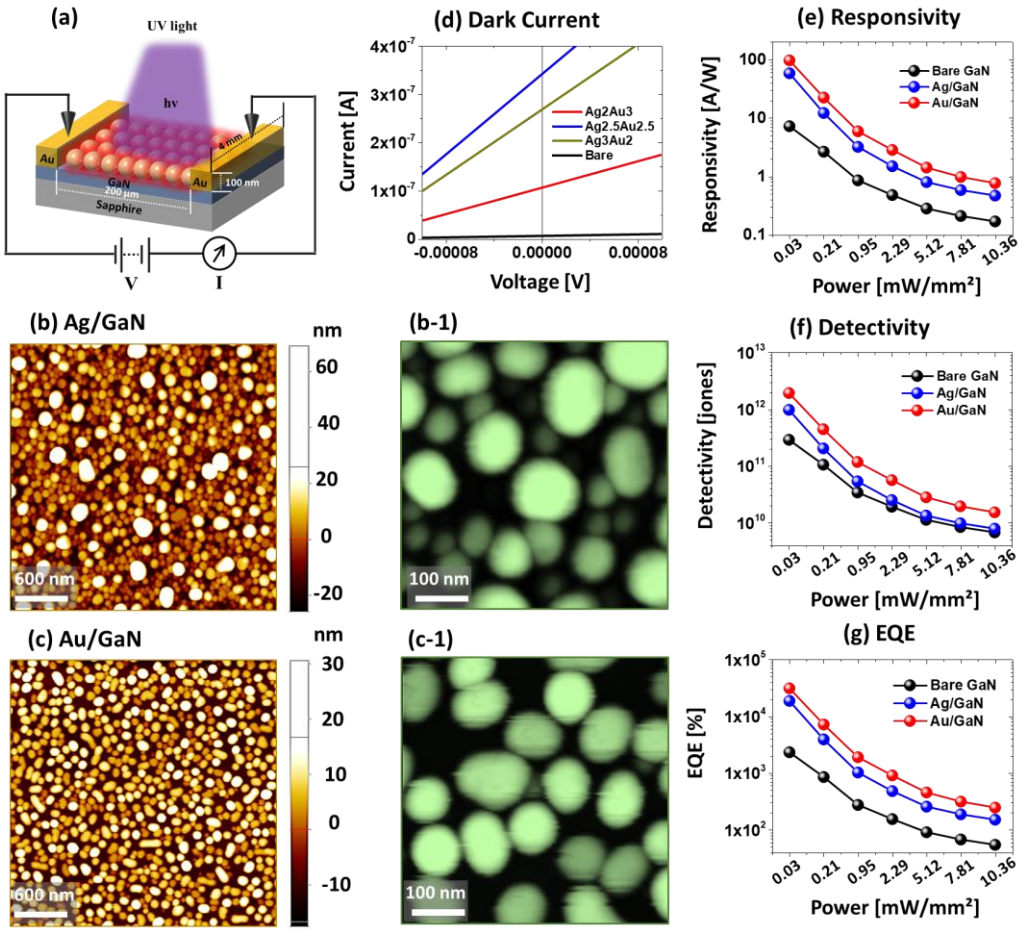

Fig. S2 a Schematic of the plasmonic NPs/GaN UV photodetector. The active region between two electrodes was 200 μm and the channel length was 4 mm and the sputtered gold electrodes were about 100 nm thick. **b-c** AFM top-views of the mono-metallic Ag and Au NPs fabricated on GaN. (**b-1**)-(**c-1**) Enlarged AFM images of the NPs. **d** Dark current of photodetector devices at low voltage range. **e-g** Summary plots of the responsivity (R), detectivity **d** and EQE of the bare GaN, Ag/GaN and Au/GaN photodetectors based on the light power variation (0.03 to 10.36 mW/mm^2). The excitation wavelength and bias voltage were 385 nm and 0.1 V respectively

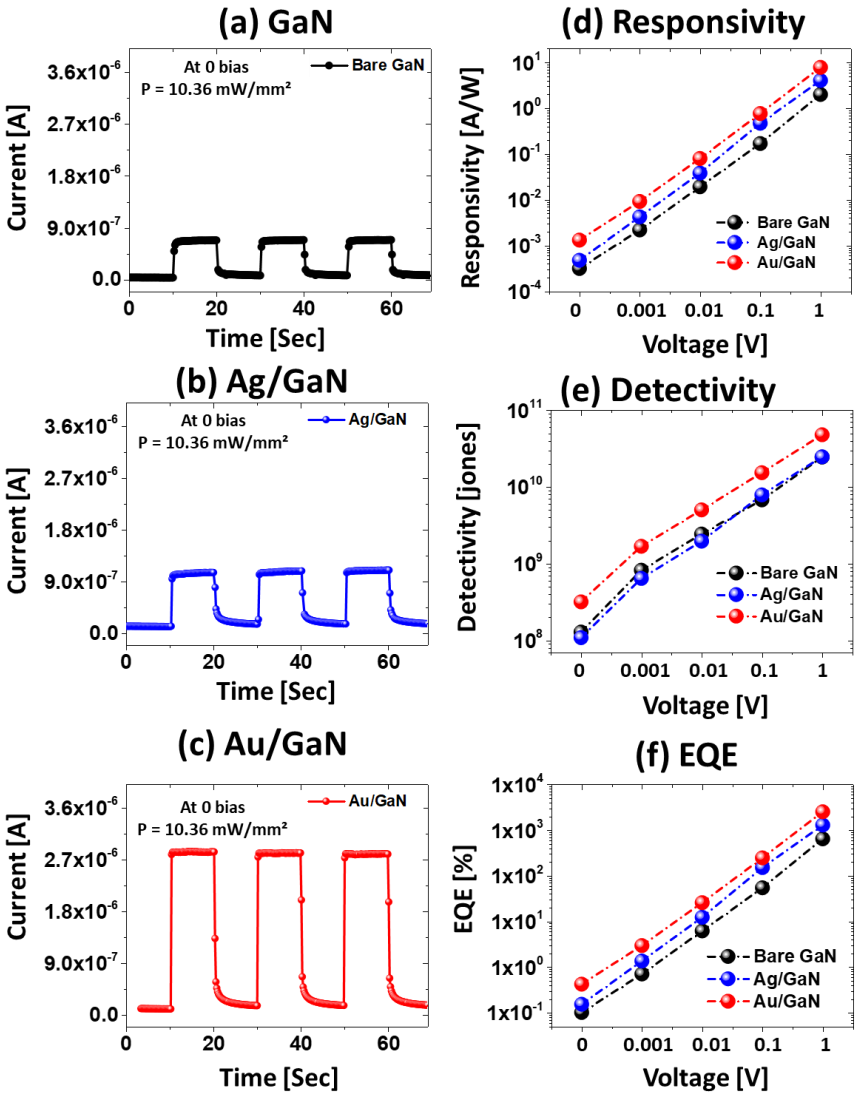

Fig. S3 a-c Photocurrent switching characteristics of the bare GaN, Ag and Au photodetectors at 0 bias upon UV on/off. The light intensity was fixed at 10.36 mW/mm^2. **d-f** Summary of the R, D and EQE of the photodetectors based on the voltage variation at constant light power of 10.36 mW/mm^2

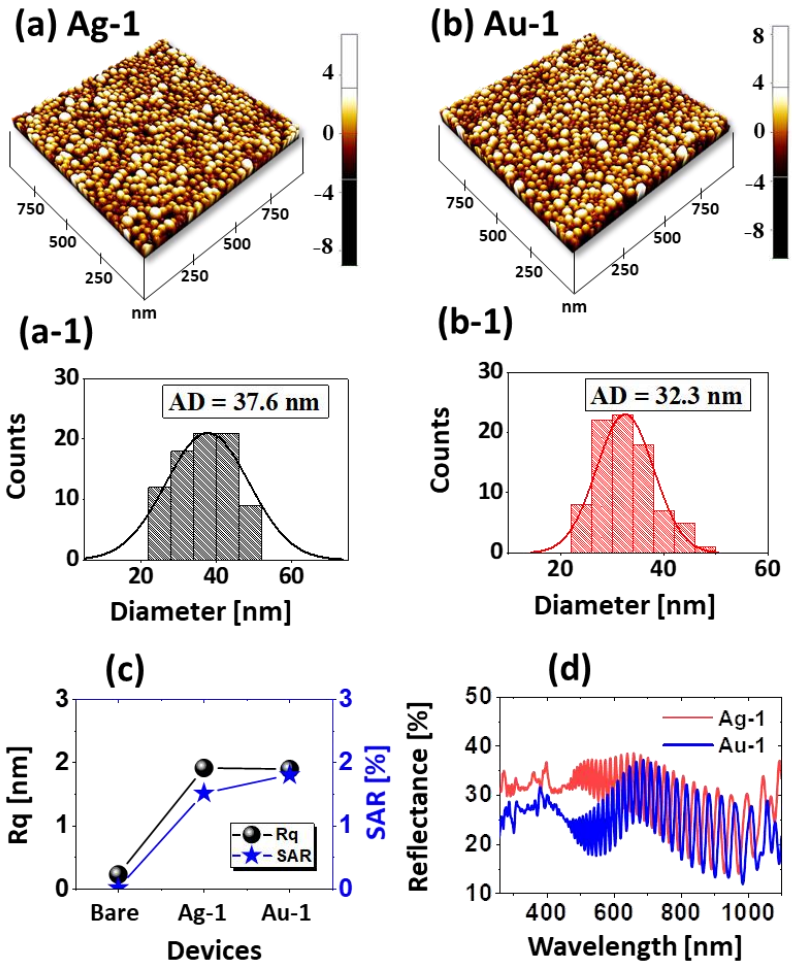

Fig S4 Fabrication of smaller size Ag and Au NPs GaN. **a-b** AFM side-views. (**a-1**)-(**b-1**) Diameter distribution histograms. **c** Summary of the RMS roughness (R_q) and surface area ratio (*SAR*). The Rq provides an average of surface profile height (y_i) as**:** $R_q = \sqrt{\frac{1}{n}\sum_{i=1}^{n} y_i^2}$. Whereas the SAR probes the increment of the 3D surface area of NPs (A_{NP}) with respect to the 2D geometric area (A_s) as: $SAR = \frac{A_s - A_{NP}}{A_s} \times 100\ \%$. **d** Reflectance spectra of Ag-1/GaN and Au-1/GaN

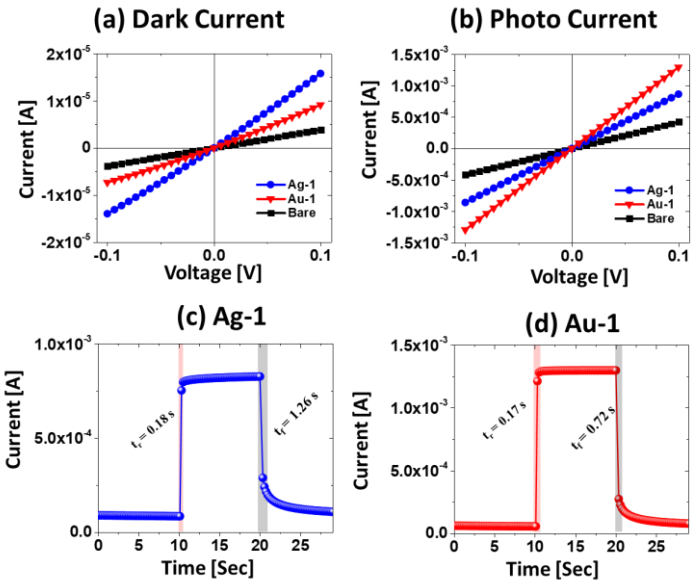

Fig. S5 Photoresponse of the small size Ag-1/GaN and Au-1/GaN NPs photodetectors. **a** *I-V* characteristic under dark. **b** Corresponding photocurrent of the devices upon illumination of UV (385 nm) at 10.36 mW mm^{-2}. **c-d** *I-t* characteristics of Ag-1/GaN and Au-1/GaN photodetectors

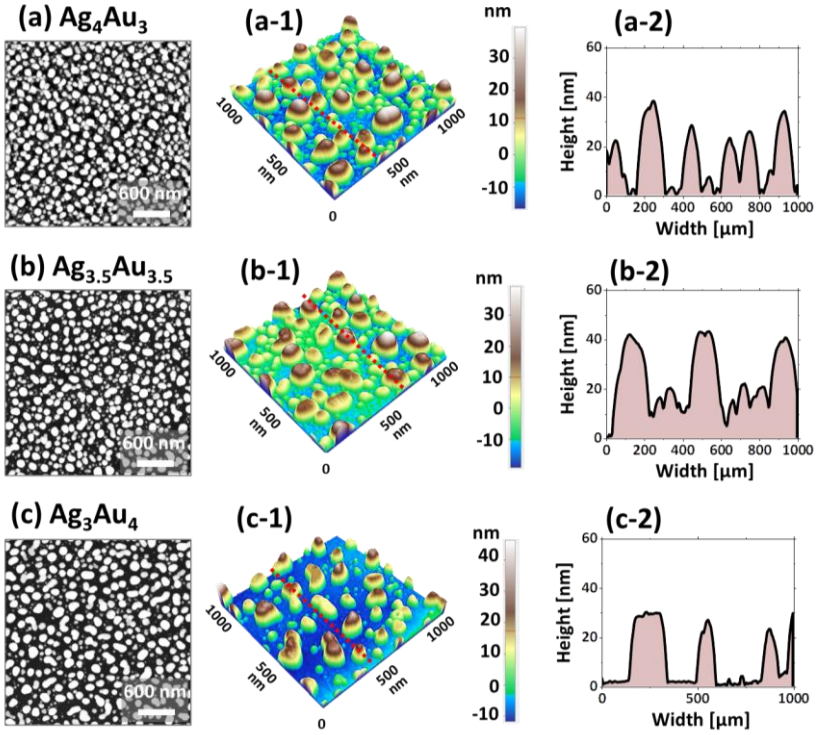

Fig. S6 a-c AFM images of the large AgAu alloy NPs fabricated on GaN with various thickness of Ag and Au in the bilayer configuration ($Ag_{x\ nm}Au_{y\ nm}$) as labelled. The AgAu alloy NPs were fabricated at 500 ºC for 60 sec. (**a-1**)-(**c-1**) Corresponding AFM side-views. (**a-2**)-(**c-2**) Cross-sectional line profiles of the AFM images in **a-c**

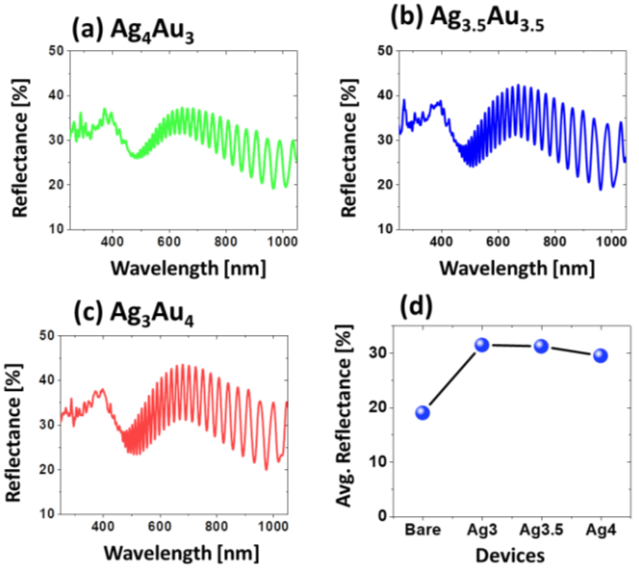

Fig. S7 a-c UV-VIS-NIR reflectance spectra of the large AgAu NPs on GaN fabricated with various initial thickness of Ag and Au. **d** Summary of the average reflectance for each sample

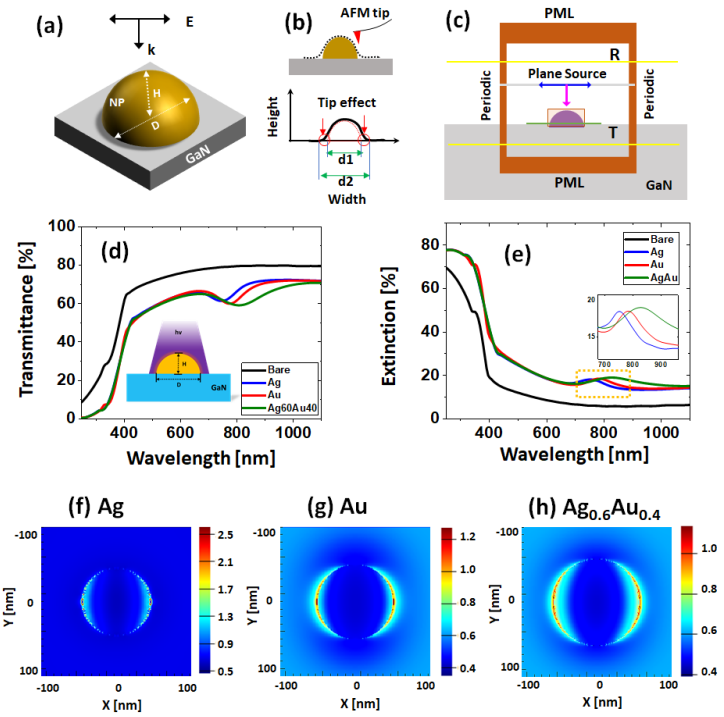

Fig. S8 a Three-dimensional model of semi-spheroid NP on GaN. **b** Diameter variation induced by the AFM tip effect. The d1 and d2 are the real and measure diameters. **c** Schematic of the finite difference time domain (FDTD) model used for the simulation. **d-e** FDTD simulated transmittance and extinction spectra of the Ag, Au and AgAu alloy NPs. **f-h** Corresponding e-field distribution of the Ag, Au and AgAu alloy NPs at 385 nm excitation

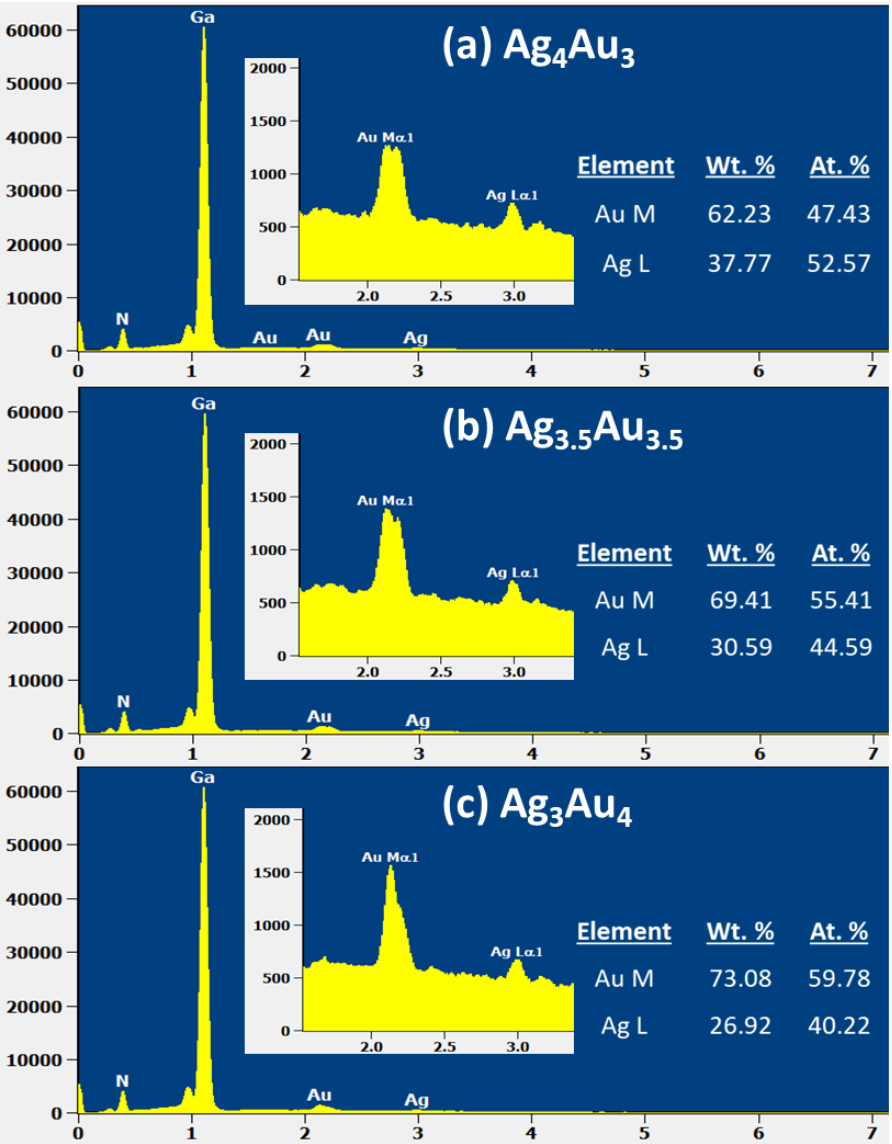

Fig. S9 a-c Energy dispersive x-ray spectroscope (EDS) spectra of the large size AgAu alloy on GaN fabricated with the various bilayer thickness of Ag and Au as labelled. The weight percentage (wt %) and atomic percentage (at%) are shown in inset tables

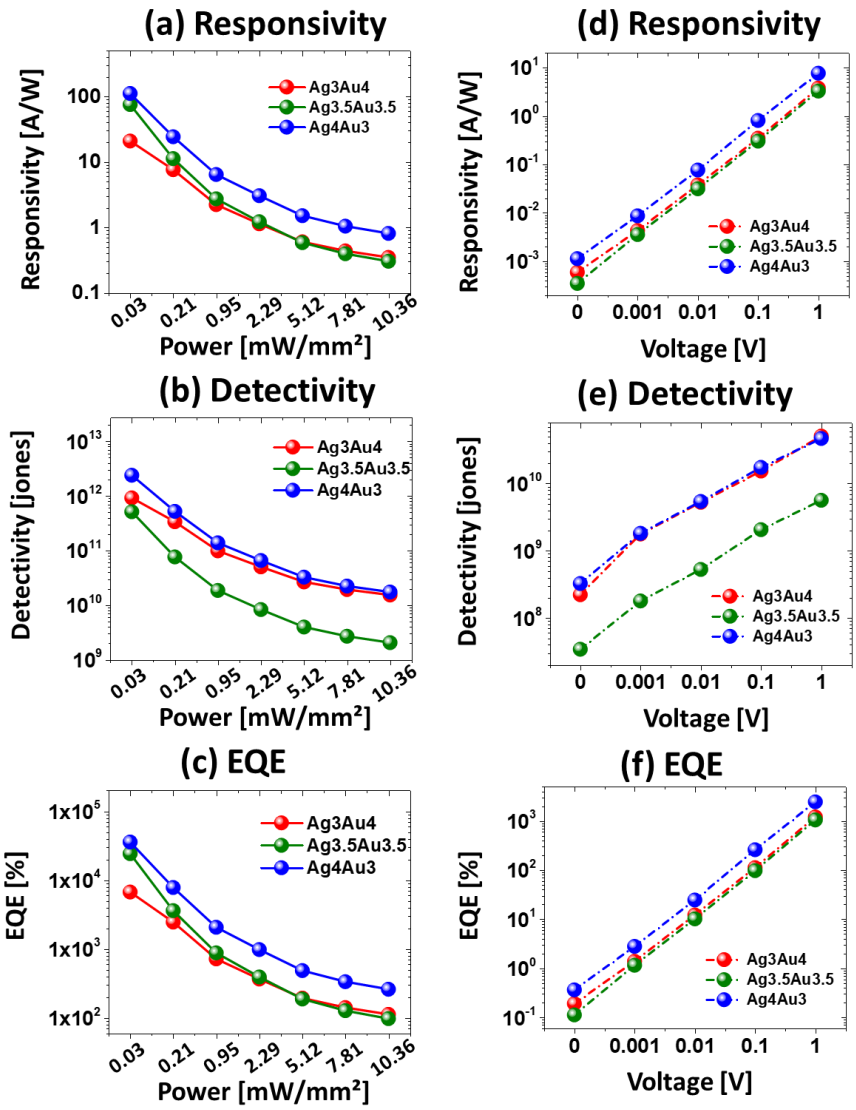

Fig. S10 a-c Summary plots of the R, D and EQE of the Ag_4Au_3/GaN, $Ag_{3.5}Au_{3.5}$/GaN and Ag_3Au_4/GaN photodetectors based on the photon power variation at fixed 0.1 V bias. **d-f** Summary of the *R*, *D* and *EQE* based on the voltage variation at fixed illumination of 385 nm at 10.36 mW mm^{-2}

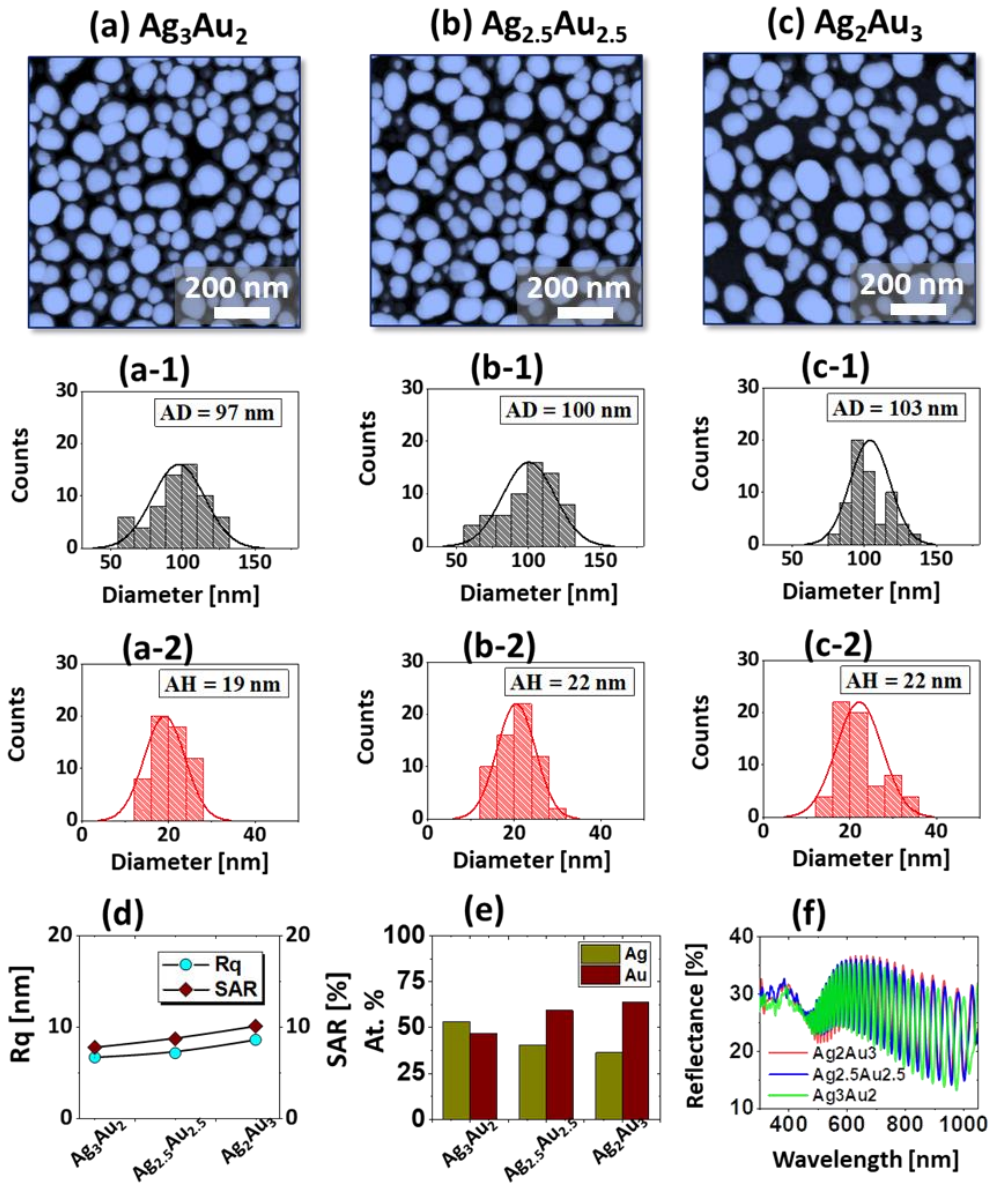

Fig. S11 Fabrication of small AgAu alloy NPs on GaN with various $Ag_{x\ nm}Au_{y\ nm}$ bilayer composition with total thickness of 5 nm by annealing at 500 ºC for 60 sec. **a** – **c** AFM top-views of the small AgAu alloy NPs. (**a-1**) – (**c-1**) Diameter distribution histogram. (**a-2**) – (**c-2**) Height distribution histogram. **d** Summary of the Rq and SAR. **e** Summary of At. % of Ag and Au in alloy NPs. **f** Reflectance spectra of the small alloy NPs

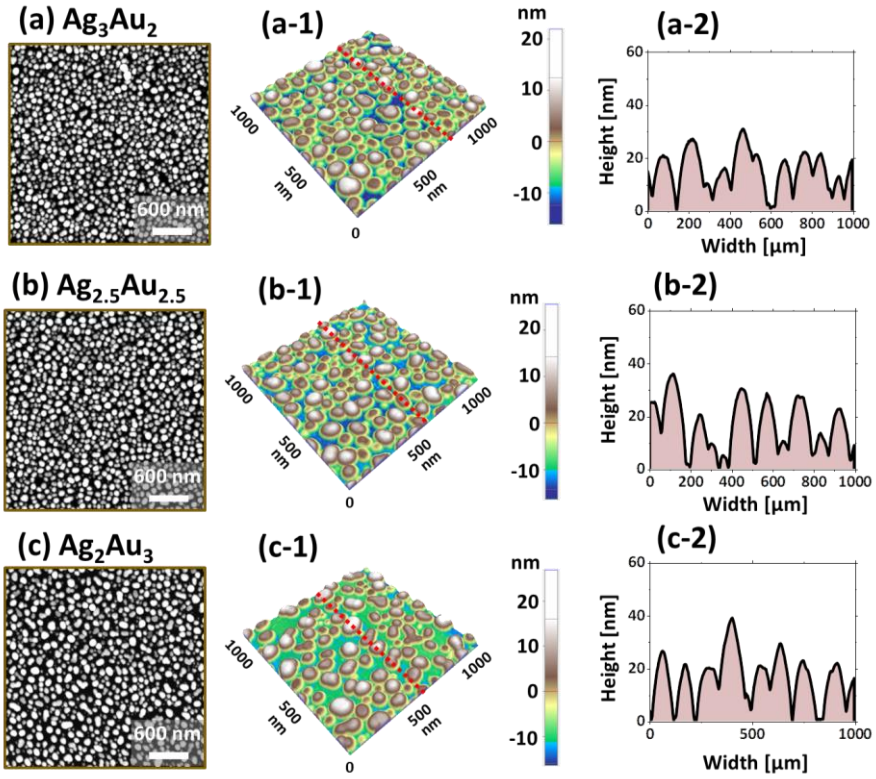

Fig. S12 a-c Large scale AFM images of the small AgAu NPs fabricated on GaN with various thickness of Ag and Au in the bilayer ($Ag_{x\ nm}Au_{y\ nm}$) as labelled. The AgAu alloy NPs were fabricated at 500 ºC for 60 sec. (**a-1**) - (**c-1**) Corresponding AFM side-views. (**a-2**) – (**c-2**) Cross-sectional line profiles of the AFM images in **a-c**

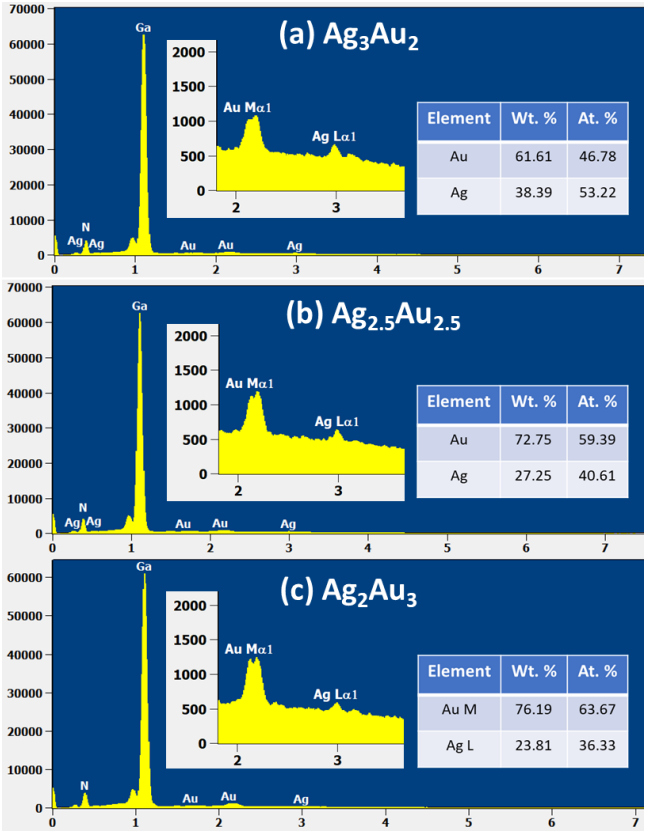

Fig. S13 a-c EDS spectra of the small size AgAu alloy on GaN fabricated with the various bilayer thickness of Ag and Au as labelled. The wt% and at% are shown in inset tables

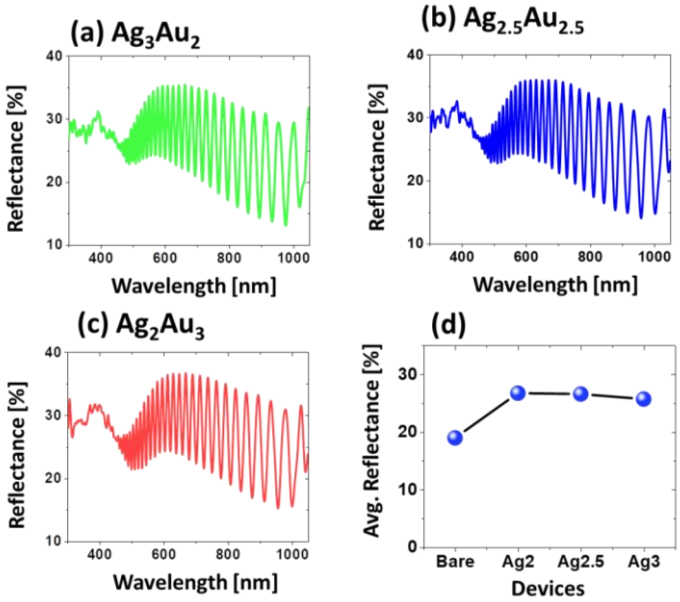

Fig. S14 a-c UV-VIS-NIR reflectance of the small AgAu NPs on GaN fabricated with various initial thickness of Ag and Au. **d** Summary of the average reflectance for various samples

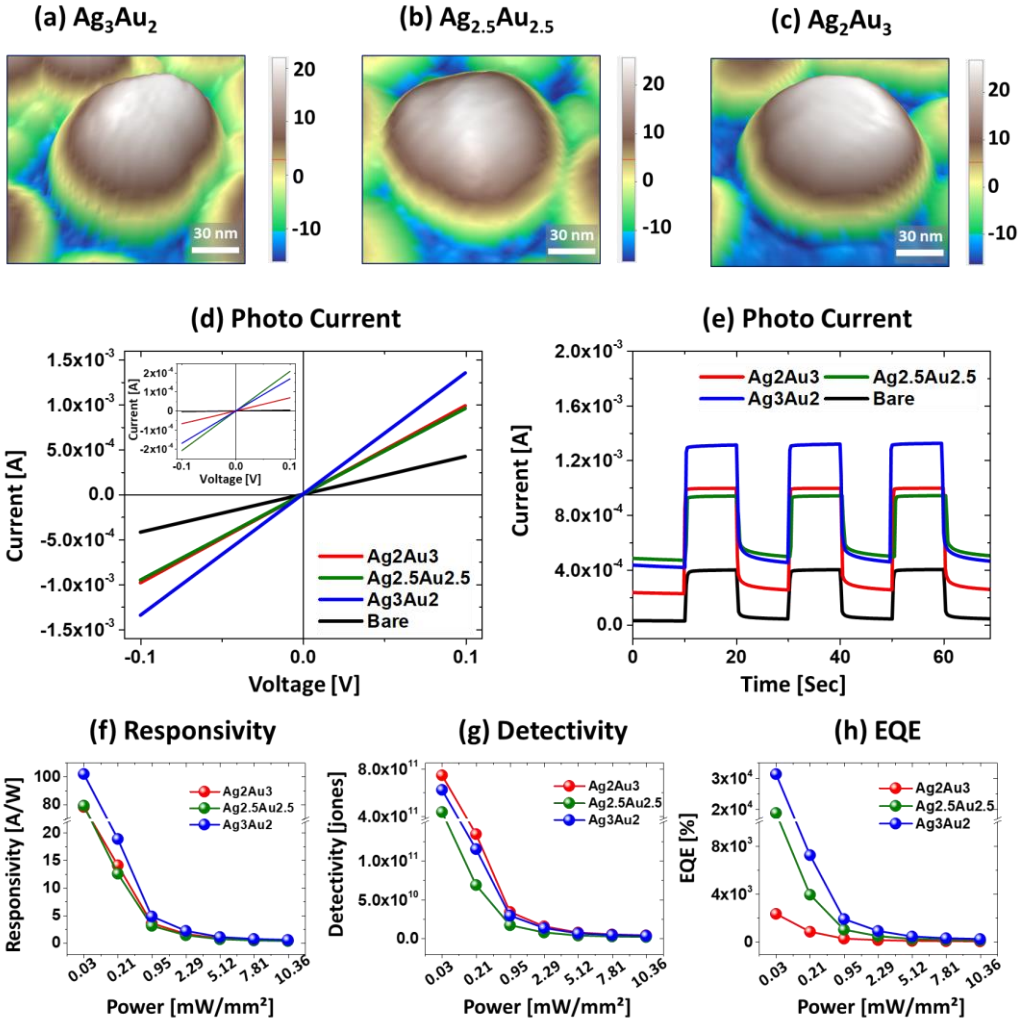

Fig. 15 a-c Typical AFM images of the small AgAu alloy NPs fabricated with various Ag_xAu_y thickness ratio on GaN as labelled. **d** *I-V* characteristic of the smaller AgAu/GaN photodetectors under 385 nm illumination at 10.36 mW mm^{-2}. The inset shows the dark current. **e** Optical switching performance of the AgAu/GaN photodetectors at 0.1 V at 10.36 mW/mm^2. **f-h** Summary plots of the R, D and EQE as function of photon power variation at 0.1 V

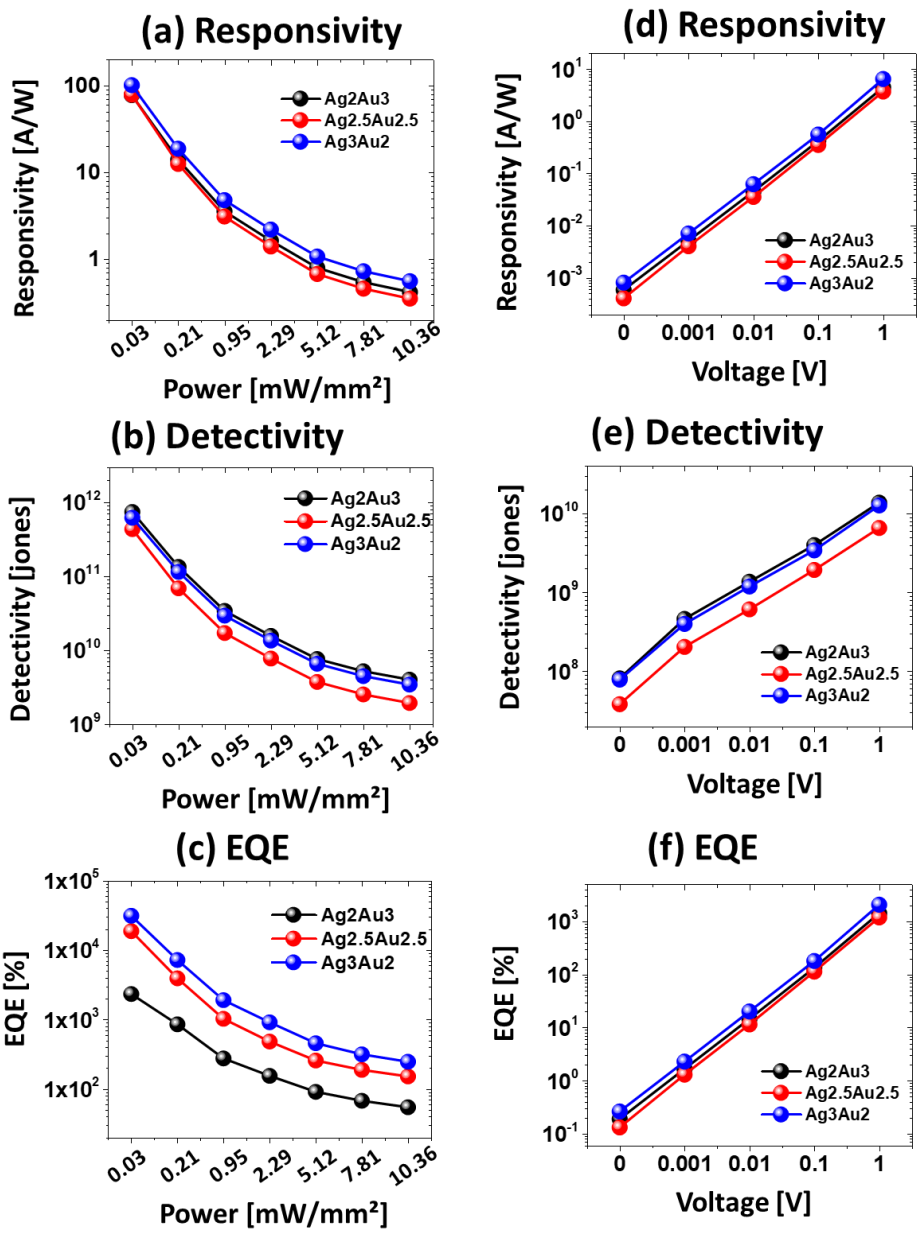

Fig. S16 a-c Summary plots of the responsivity, detectivity and EQE of the Ag_3Au_2/GaN, $Ag_{2.5}Au_{2.5}$/GaN and Ag_2Au_3/GaN photodetectors based on the light intensity variation at fixed 0.1 V bias. **d-f** Summary of the responsivity, detectivity and EQE based on the voltage variation at fixed illumination of 385 nm at 10.36 mW mm^{-2}

Table S1 Summary of the average diameter (AD) and height (AH) of various mono-/bi-metallic NPs fabricated on GaN

Samples	**AD [nm]**	**AH [nm]**	R_q **[nm]**	**SAR [%]**
Ag/GaN	102	27	13.23	13.93
Au/GaN	105	25	8.23	10.40
Ag-1/GaN	37.6	6	1.91	1.80
Au-1/GaN	32.3	8	1.89	1.51
Ag4Au3/GaN	114	26	11.44	15.86
Ag3.5Au3.5/GaN	116	27	10.95	14.19
Ag3Au4/GaN	118	30	11.04	13.67
Ag3Au2/GaN	97	19	8.58	10.08
Ag2.5Au2.5/GaN	100	22	7.13	8.69
Ag2Au3/GaN	103	22	6.67	7.76

Table S2 Summary of the responsivity (R), detectivity (D) and external quantum efficiency (EQE) of the bare GaN, Ag, Au photodetectors as function of illumination power variation at a constant bias of 0.1 V

Power [mW/mm^2]	**Responsivity [A/W]**			**Detectivity [Jones]**			**EQE [%]**		
	GaN	**Ag**	**Au**	**GaN**	**Ag**	**Au**	**GaN**	**Ag**	**Au**
0.03	7.26	58.5	97.4	2.91E+11	9.83E+11	1.94E+12	2339	18800	31370
0.21	2.66	12.2	22.5	1.07E+11	2.06E+11	4.48E+11	855	3940	7230
0.95	0.86	3.21	5.97	3.44E+10	5.40E+10	1.18E+11	276	1030	1911
2.29	0.48	1.5	2.8	1.93E+10	2.53E+10	5.67E+10	155	484	916
5.12	0.28	0.802	1.4	1.14E+10	1.35E+10	2.83E+10	91	258	457
7.81	0.20	0.586	0.9	8.45E+09	9.86E+09	1.96E+10	67	189	316
10.36	0.17	0.471	0.7	6.81E+09	7.92E+09	1.54E+10	54	152	247

Table S3 Summary of the *R*, *D* and *EQE* of the bare GaN, Ag, Au based on the bias variation at 10.36 mW/mm^2

Voltage [V]	Responsivity [A/W]			Detectivity [Jones]			EQE [%]		
	GaN	**Ag**	**Au**	**GaN**	**Ag**	**Au**	**GaN**	**Ag**	**Au**
0	3.16E-4	4.78E-4	0.00132	1.29E+08	1.09E+08	3.19E+08	0.102	0.154	0.425
0.001	0.0022	0.00425	0.00923	8.25E+08	6.45E+08	1.69E+09	0.71	1.37	2.97
0.01	0.0193	0.0384	0.0803	2.44E+09	1.97E+09	5.04E+09	6.22	12.4	25.9
0.1	0.17	0.471	0.77	6.81E+09	7.92E+09	1.54E+10	54.8	152	248
1	2.01	4.05	7.88	2.46E+10	2.48E+10	4.81E+10	648	1300	2540

Table S4 Summary of the *R*, *D* and *EQE* of the Ag_4Au_3, $Ag_{3.5}Au_{3.5}$, Ag_3Au_4 as function of illumination power variation at a constant bias of 0.1 V

Power [mW/mm^2]	Responsivity [A/W]			Detectivity [Jones]			EQE [%]		
	Ag_4Au_3	**$Ag_{3.5}Au_{3.5}$**	**Ag_3Au_4**	**Ag_4Au_3**	**$Ag_{3.5}Au_{3.5}$**	**Ag_3Au_4**	**Ag_4Au_3**	**$Ag_{3.5}Au_{3.5}$**	**Ag_3Au_4**
0.03	112	75.8	48.4	2.40E+12	5.15E+11	2.14E+12	36000	24400	15600
0.21	24.4	11.3	8.84	5.25E+11	7.67E+10	3.90E+11	7860	3630	2850
0.95	6.47	2.75	2.5	1.39E+11	1.87E+10	1.10E+11	2080	885	804
2.29	3.07	1.23	1.22	6.60E+10	8.34E+09	5.37E+10	988	395	392
5.12	1.52	0.588	0.613	3.27E+10	4.00E+09	2.70E+10	489	189	197
7.81	1.05	0.398	0.44	2.25E+10	2.71E+09	1.94E+10	337	128	142
10.36	0.814	0.305	0.35	1.75E+10	2.07E+09	1.54E+10	262	98.1	113

Table S5 Summary of the *R*, *D* and *EQE* of the Ag_4Au_3, $Ag_{3.5}Au_{3.5}$, Ag_3Au_4 photodetectors with the large size NPs as function of bias variation at 10.36 mW/mm^2

Voltage [V]	Responsivity [A/W]			Detectivity [Jones]			EQE [%]		
	Ag_4Au_3	$Ag_{3.5}Au_{3.5}$	Ag_3Au_4	Ag_4Au_3	$Ag_{3.5}Au_{3.5}$	Ag_3Au_4	Ag_4Au_3	$Ag_{3.5}Au_{3.5}$	Ag_3Au_4
0	5.96E-4	3.5E-4	0.00114	3.27E+08	3.44E+07	2.23E+08	0.366	0.113	0.192
0.001	0.00435	0.00359	0.00872	1.83E+09	1.80E+08	1.78E+09	2.81	1.16	1.4
0.01	0.0381	0.0316	0.0771	5.45E+09	5.30E+08	5.28E+09	24.8	10.2	12.3
0.1	0.35	0.305	0.814	1.75E+10	2.07E+09	1.54E+10	262	98.1	113
1	3.8	3.29	7.69	4.71E+10	5.67E+09	5.11E+10	2480	1060	1220

Table S6: Summary of the *R*, *D* and *EQE* of the Ag_3Au_2, $Ag2_{.5}Au_{2.5}$, Ag_2Au_3 photodetectors with the smaller size NPs as function of illumination power variation at a constant bias of 0.1 V

Power [mW/mm^2]	Responsivity [A/W]			Detectivity [Jones]			EQE [%]		
	Ag_3Au_2	$Ag_{2.5}Au_{2.5}$	Ag_2Au_3	Ag_3Au_2	$Ag_{2.5}Au_{2.5}$	Ag_2Au_3	Ag_3Au_2	$Ag_{2.5}Au_{2.5}$	Ag_2Au_3
0.03	102	79.3	78.3	6.22E+11	4.35E+11	7.45E+11	32900	25500	25219
0.21	18.9	12.6	14.11	1.15E+11	6.88E+10	1.34E+11	6080	4050	4543
0.95	4.83	3.12	3.6	2.94E+10	1.71E+10	3.41E+10	1550	1000	1154
2.29	2.21	1.41	1.64	1.35E+10	7.72E+09	1.56E+10	711	454	529
5.12	1.08	0.679	0.8	6.56E+09	3.72E+09	7.62E+09	347	219	257
7.81	0.731	0.46	0.55	4.46E+09	2.52E+09	5.20E+09	236	148	175
10.36	0.561	0.353	0.4	3.42E+09	1.93E+09	4.00E+09	181	114	135

Table S7 Summary of the *R*, *D* and *EQE* of the bare Ag_3Au_2, $Ag2.5Au2.5$, Ag_2Au_3 photodetectors with smaller size NPs as function of bias variation at a constant power of10.36 mW/mm^2

Voltage [V]	Responsivity [A/W]			Detectivity [Jones]			EQE [%]		
	Ag_3Au_2	$Ag_{2.5}Au_{2.5}$	Ag_2Au_3	Ag_3Au_2	$Ag_{2.5}Au_{2.5}$	Ag_2Au_3	Ag_3Au_2	$Ag_{2.5}Au_{2.5}$	Ag_2Au_3
0	8.12E-4	4.06E-4	5.87E-4	7.85E+07	3.83E+07	8.15E+07	0.262	0.131	0.189
0.001	0.00711	0.00404	0.00517	3.99E+08	2.04E+08	4.62E+08	2.29	1.3	1.67
0.01	0.0627	0.0356	0.0454	1.19E+09	6.11E+08	1.37E+09	20.2	11.5	14.6
0.1	0.561	0.353	0.421	3.42E+09	1.93E+09	4.00E+09	181	114	135
1	6.5	3.73	4.48	1.27E+10	6.58E+09	1.38E+10	2090	1200	1440